

Studies of non-linear bubble oscillations in a simulated acoustic field

T G Leighton, M Wilkinson, A J Walton and J E Field

Cavendish Laboratory, Madingley Road, Cambridge CB3 0HE, UK

Received 22 January 1990, in final form 30 May 1990

Abstract. Gas bubbles in liquids are capable of forced oscillations in a sound field. Photographic study of these non-linear oscillations is difficult. It is technically most feasible at low acoustic frequencies, where lower framing rates are required, and where the resonance bubble size is larger. However, the acoustic pressures required to elicit a non-linear response from the bubble might, if generated at audible frequencies, be damaging to the hearing. This paper outlines an experimental solution to the problem, whereby a volume of liquid containing bubbles is vibrated vertically. The oscillating pressure in the water mimics an acoustic field at the vibration frequency and the bubble responds to it as such. The apparatus has minimal audible emissions, yet the oscillating pressure is of such an amplitude as to generate highly non-linear oscillations in the bubble. The experiment provides a good example of forced oscillation, as well as illustrating a subtle solution to a difficult experimental problem. Radius-time data from a given bubble were obtained using high-speed and stroboscopic photography, and were compared with the numerical predictions obtained from the Rayleigh-Plesset equation.

Résumé. Des bulles de gaz dans les liquides peuvent présenter des oscillations forcées dans un champ acoustique. L'étude photographique de ces oscillations non linéaires est difficile.

C'est techniquement le plus aisé aux fréquences acoustiques quand une vitesse de prise de vue plus basse est nécessaire et la dimension des bulles en résonance est plus grande. Cependant, les pressions acoustiques nécessaires pour susciter une réponse non linéaire d'une bulle peuvent, si elles sont générées à des fréquences audibles, endommager le système auditif.

Cet article décrit pour ce problème une solution expérimentale dans laquelle le liquide qui contient les bulles vibre verticalement. La pression oscillante dans l'eau est l'analogie d'un champ acoustique à la fréquence de vibration, auquel la bulle réagit.

L'appareil a un minimum d'émission dans le domaine audible et cependant la pression oscillante est d'une amplitude telle qu'elle génère des oscillations hautement non linéaires dans la bulle. L'expérience fournit un bon exemple d'oscillation forcée, de même qu'elle illustre une solution subtile d'un problème expérimental difficile.

Les mesures rayon-temps pour une bulle donnée sont obtenues en utilisant la photographie stroboscopique à haute vitesse et sont comparées aux prédictions numériques obtenues à partir de l'équation de Rayleigh-Plesset.

1. Introduction

A spherical gas bubble within a liquid may perform volume pulsations, which can be either free or forced. The free oscillations were first studied by Minnaert (1933) given a mechanical exciting impulse, the amplitude of oscillation of the bubble wall is small, and so the bubble approximates to a linear oscillator. The pulsations occur at a well defined resonance frequency ν_r , given approximately by

$$\nu_r = (1/2\pi R_0)(3KP_0/\rho)^{1/2} \quad (1)$$

where R_0 is the equilibrium bubble radius, ρ is the liquid density, P_0 is the ambient hydrostatic pressure

and K is the so-called polytropic index (which takes a value between unity and γ depending on whether the gas is behaving isothermally, adiabatically, or in some intermediate manner). For air bubbles in water under one atmosphere, equation (1) reduces to

$$\nu_r R_0 \approx 3 \text{ Hz m} \quad (2)$$

The acoustic output of such a freely oscillating bubble is typically an exponentially decaying sinusoid, which has been recorded in the sound of many phenomena, including the babbling of brooks (Leighton and Walton 1986) and the impact of water drops on a body of liquid, the 'noise of a dripping tap' (Pumphrey and Walton 1988).

As with any oscillating system, the bubble may also be driven into oscillation, for example by being subjected to a periodic driving pressure in the form of an acoustic wave. At low acoustic pressure amplitudes, the radial oscillation is small and the bubble response approximates to the familiar form of the lightly damped simple harmonic oscillator. Higher acoustic driving pressures can give rise to non-linear oscillations in the bubble, the amplitude of oscillation of the bubble wall now being higher. Though the equations of motion of the bubble are awkward (Neppiras 1980), the forced bubble provides a good example of a non-linear oscillator. In simple terms the non-linearity arises because though there are no limits to the radius in expansion, the amplitude of the radial decrease in contact is limited. One of the most common of these equations of motion is the Rayleigh-Plesset (also called the $R\ddot{P}NNP$) equation for a single bubble in an infinite medium

$$R\ddot{R} + 3\dot{R}^2/2 = (1/\rho)[(P_0 + 2\sigma/R_0 - P_v)(R_0/R)^{3\lambda} - 2\sigma/R - 4\mu\dot{R}/R - P_0 - P(t)] \quad (3)$$

where $R(t)$ is the bubble radius, σ the surface tension, μ the viscosity of the liquid and $P(t)$ the time-varying pressure component (i.e. the forcing term). An outline of the derivation of this equation can be found in Leighton *et al* (1990). When the surface tension and viscosity terms in the Rayleigh-Plesset equation are deemed negligible, the formulation can be reduced to give equation (1).

The interaction of sound with bubbles as it passes through liquid is of importance in two general fields: medical ultrasound and underwater communications. The former employs acoustic frequencies of the order of MHz, whilst the latter uses kHz. Equation (2) shows that the bubble radius resonant with these frequencies are of magnitude 10^{-6} m and 10^{-4} m respectively. Due to the small size and rapid motions of these bubbles, it is very difficult to image them directly and one is often forced to rely upon numerical solutions to the equations of motion to predict the oscillatory motion of such bubbles.

If millimetre-sized bubbles are insonated at low acoustic frequencies, photographic observations of the radial motion are much easier. However, the high-intensity sound fields required to produce non-linear effects at audible frequencies represent a hazard to hearing. A system has therefore been designed that produces a low-frequency oscillatory pressure field without audible emissions.

In this study, high-speed and stroboscopic photography were used to obtain radius-time data for bubbles within an oscillatory high-amplitude pressure field. These data were then compared with the Rayleigh-Plesset predictions. The photographic evidence was also used to interpret to what extent certain effects (such as non-sphericity) affect the motion, and gives direct information about the validity of the Rayleigh-Plesset equation in this regime.

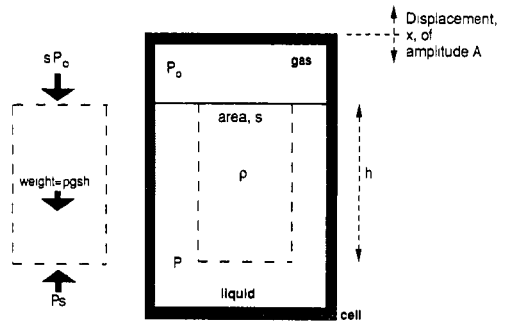


Figure 1 Schematic diagram of the vibrated liquid, with the forces acting on the liquid column indicated.

2. Experimental

The method used to produce an intense oscillating pressure field is to vibrate a vertical tube of liquid at a set frequency ω and with an amplitude of oscillation A . An acoustic frequency of 100 Hz is used. This is lower than those encountered in the applications mentioned above, but it facilitated the high-speed photography. The 100 Hz oscillation allowed sufficient data points to be taken per cycle to satisfy the Nyquist criterion. Also, the resonance bubble radius is larger, reducing the need for high optical magnification.

To produce the oscillating pressure field at these audio frequencies without causing discomfort, the liquid containing the bubble was vibrated vertically at frequency ω (see figure 1). If x is the vertical displacement of the cell from equilibrium, of amplitude A , then

$$x = A \sin \omega t \quad (4)$$

and

$$(d^2x/dt^2) = -A\omega^2 \sin \omega t \quad (5)$$

Consider a vertical column within the liquid, with a cross-sectional area s and a length h , which extends down from the liquid surface (figure 1). Then if ρ is the liquid density, g the acceleration due to gravity, P_0 the pressure above the liquid, and P the pressure at a distance h below the liquid surface, then from Newton's second law,

$$(P - P_0)s - \rho ghs = \rho sh(d^2x/dt^2) \quad (6)$$

Rearrangement of this, and substitution from equation (5) gives

$$P = (P_0 + \rho gh) - \rho A\omega^2 h \sin \omega t \quad (7)$$

This expression corresponds to an oscillating pressure of amplitude $(\rho A\omega^2 h)$ and frequency ω , superimposed on a static pressure of $(P_0 + \rho gh)$. Generally, the larger the static pressure at a bubble, the smaller

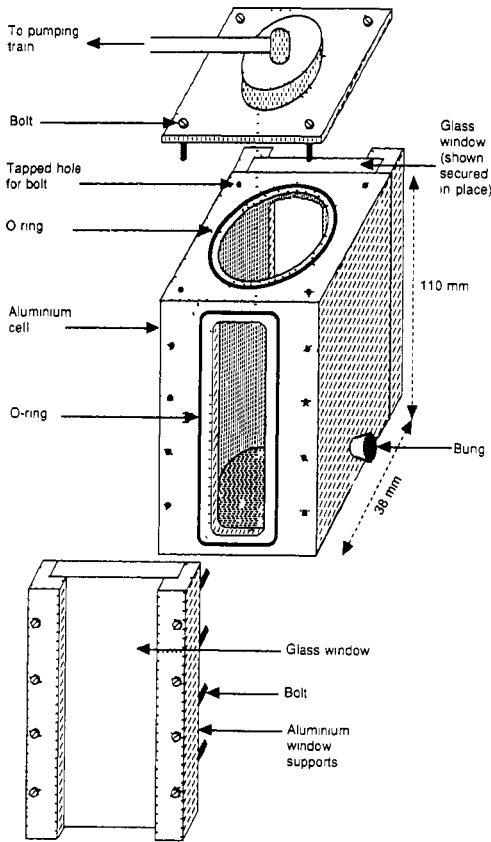


Figure 2 Schematic diagram of the cell used to contain the liquid under reduced pressure

the amplitude of the radial oscillations. Thus to obtain high-amplitude, and therefore non-linear, bubble pulsations in the simulated acoustic field, the quantity $(P_0 + \rho gh)$ must be minimised. This is done experimentally by reducing the pressure head P_0 above the liquid.

The apparatus is shown in figures 2 and 3. The test liquid is placed, to a level of about $3/4$, in the cell which is shown partly assembled in figure 2. This cell consists basically of an aluminium rectangular block, into which a cylindrical hole has been drilled, parallel to the long axis. The diameter and length of this cavity are 27 mm and 90 mm respectively. Two window holes are milled into opposing sides of the block and are covered with glass plates, secured in place by aluminium brackets. An O-ring, set in a milled groove around the window, improves the vacuum-tightness. A similar O-ring is used to keep air-tight the joint with the top-plate, which houses the valve system and the piping that leads to the pumping train. The cell is pumped down to about 100 Pa, and placed upon a

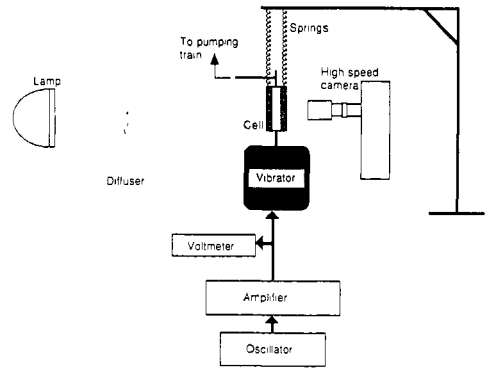


Figure 3. Schematic diagram of the experimental arrangement

vibrator (Goodmans Industries type 390, figure 3). Extended springs attached to the top of the cell pull up against its weight, so that at rest the cell lies at the equilibrium position of the vibrator. Without these springs, the vibrator bottoms out at high amplitude, and the motion ceases to be sinusoidal. The vibrator is driven by an electrical sinusoid at 100 Hz from a Brookdeal Signal Source (type 471), which is amplified by a Quad 510 power amplifier (capable of generating 135 W at audio frequencies). A voltmeter is used to ensure a reproducible signal.

The initial studies were performed using variably delayed stroboscopic photography. Once the bubble has settled down to steady-state motion, the delay of the stroboscope could be altered to scan through the oscillatory cycle, enabling a complete study of the bubble motion to be recorded using stills photography. The stroboscope was triggered by taking a signal from the vibrator input. A computer program was written to control the camera and the delay, greatly increasing the speed of the observations. A similar system could be developed for conventional flash photography by gating a synchronisation signal derived from the vibrator input with the camera's flash socket. A variable delay applied to the gate output would then be used to trigger the flash.

With stills photography, the buoyant rise of bubbles can also create problems in keeping the subject within the field of view. High-speed photography solves this problem, and also allows data to be taken on a bubble before it has settled down to the steady-state. A Hadland Hyspeed rotating prism camera was used, operating at 2000 frames per second (fps) and with a field of view of 4 mm \times 6 mm. Two 800 W 'red-head' spotlights behind a diffusing screen provided illumination (figure 3). Cine film (16 mm, 400 ASA) was used in 30 m reels, taking typically 2 s of continuous photography. The film was developed in ID11 at 20°C for 12 minutes. An internal strobe spot-marked the film with an accurate timing light to

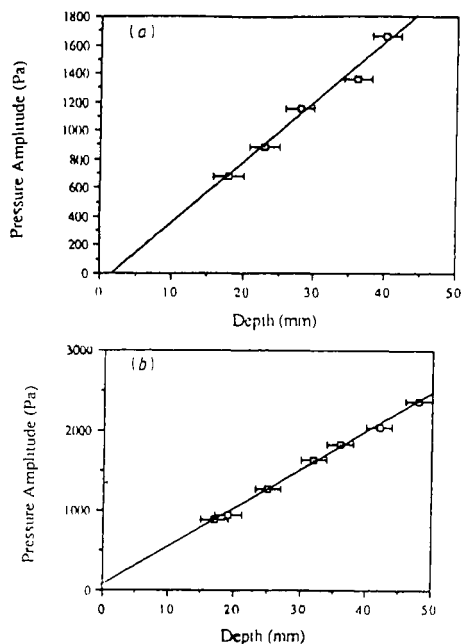


Figure 4 Graphs of experimentally measured acoustic pressure amplitude (\square) against that predicted by equation (7) (a) water and (b) glycerol

record on the film itself the instantaneous framing rate

Tap water and glycerol were used as test liquids. At high pressure amplitudes bubbles tended to grow by rectified diffusion (Walton and Reynolds 1984) from nucleation sites within the liquid. However, more controllable bubble production was achieved by injecting air into the cell at a steady rate using a syringe needle, inserted through a bung in the side of the cell (figure 2). In fact, the suction from the reduced pressure drew in air adequately through the needle, making the syringe itself redundant. Withdrawing the needle tip into the body of the bung reduced the bubble production rate further.

The effective pressure amplitude (the term $\rho A \omega^2 h$ in equation (7)) was found in two ways. Firstly, each of the parameters in the expression was directly measured, enabling the product to be calculated. To find A , the cell was illuminated by a stroboscope, at frequency ω , so freezing its visible motion. By varying the phase delay, the complete path of the cell could be examined. This method could also be used to check that the vibration of the cell was sinusoidal, and not subject to 'bottoming out'. Instead of using a variable phase-delay system, the frequency of the strobe can alternatively be set to be slightly different from ω , the frequency of the vibrator. Secondly, the top of the cell can be removed (the system would then not be under reduced pressure) and a hydrophone (Bruel and Kjaer

type 8103) inserted into the liquid. Knowing the calibration of the hydrophone, the pressure amplitude can be found from the hydrophone output as monitored by an oscilloscope. To check that there was no electromagnetic pickup by the hydrophone from the vibrator, this procedure was repeated in the absence of the test liquid: no signal was seen, proving the previous measurement of pressure amplitude genuine. Both results for pressure amplitude are shown in figure 4, where the agreement of the measured values with those calculated by the product $\rho A \omega^2 h$ is clear.

When a film was taken, the camera was initially started whilst the vibrator was stationary. This allowed the bubbles to be photographed whilst non-oscillatory, permitting their equilibrium radius to be subsequently measured. After a few tenths of a second, the vibrator was started. The bubble motion therefore is that of an initially stationary bubble suddenly subjected to an oscillatory pressure field (i.e. at $t = 0$, $R = R_0$ and $\{dR/dt\} = 0$). The developed film was projected onto a screen, giving an overall linear magnification of camera plus projector of about 100. Frame-by-frame analysis of the film gave data for the bubble radius as a function of time, and these were compared with the computer predictions. Since these numerical solutions assume that insonation begins at $t = 0$, it is necessary to relate the experimental data to that time when the pressure oscillations began. Experimentally, the time t after the start of insonation could be measured directly if the bubble had been in the field of view at $t = 0$. If it had not been visible at $t = 0$, but had later risen into the picture, the time that the bubble had been present in the sound field could be estimated from its measured velocity on the film.

The bubbles photographed were all near, but less than, resonance size. This can be seen by substituting typical values of the required parameters into equation (1). With an acoustic frequency of $\nu = 100$ Hz, and with $P_0 = 600$ Pa, $\rho = 1000$ kg m $^{-3}$, and $K = 1.33$, we obtain a resonant equilibrium bubble radius of $R_0 = 2.5$ mm. Ideally it would have been useful to employ higher acoustic frequencies in addition to the 100 Hz used here, to drive the bubbles closer to resonance. This, however, was not possible due to the limitations of the vibrator. Nevertheless, 100 Hz proved to be a useful compromise. The driving frequency and static pressure were not varied, but a range of equilibrium bubble radii was studied. The test liquid was either water or glycerine, and the acoustic pressure amplitude was controlled and varied.

Numerical solutions to the Rayleigh-Plesset equation were found using FORTRAN on the Cambridge University IBM 3084 mainframe. The equation was split into a system of first-order ordinary differential equations and solved by the NAG routine D02CBF, which employs a variable-order variable-step Adams method. The boundary conditions matched the experimental ones (i.e. at $t = 0$, $R = R_0$ and $\{dR/dt\} = 0$). The output shows the bubble radius, the wall velocity, and the internal pressure and

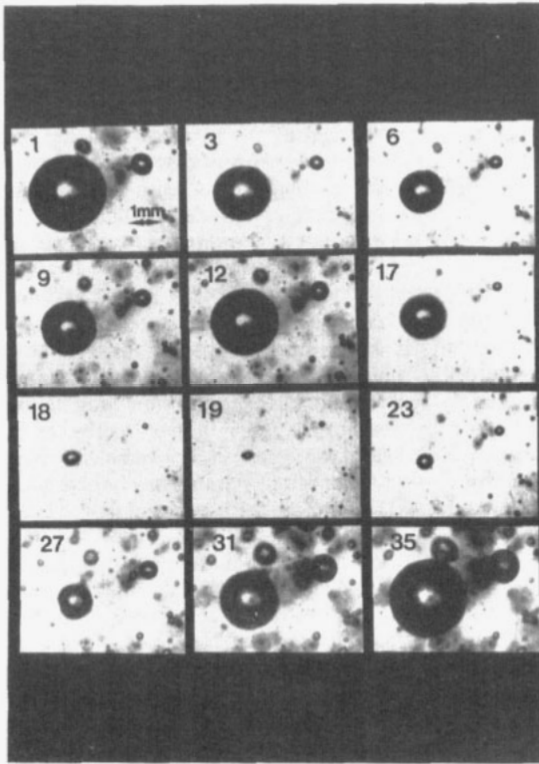


Figure 5. A selection of frames from a sequence of 35 consecutive frames, filmed at 2000 fps, showing stable air bubble oscillation in glycerol. The acoustic frequency is 100 Hz, the static pressure 600 Pa, and the acoustic pressure amplitude 3900 Pa. The radius-time data from this set of pictures is compared with the theoretical predictions in figure 9. The bubble contracts to reach a minimum in frame 6, expands to a maximum in frame 12, then collapses to a smaller minimum in frame 19. This second collapse is gradual to frame 17, then becomes very rapid.

temperature within the bubble as a function of time.

3. Results

Examples of the photographic results are shown in figures 5 to 7. Each corresponds to a selection of frames from the complete film record. The time between consecutively numbered frames is 500 μ s. Figure 5 shows an air bubble in glycerine under high pressure amplitude (3900 Pa), with a static pressure of 600 Pa. The selected frames show non-linear oscillation of the main bubble. From frame 1, it contracts to a minimum size in frame 6, then expands to a maximum in frame 12. The subsequent collapse is gradual until frame 17, from which point onwards the collapse is very rapid, attaining a much smaller minimum volume in frame 19. The expansion is then gradual to

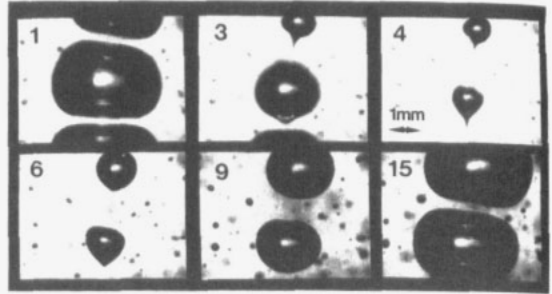
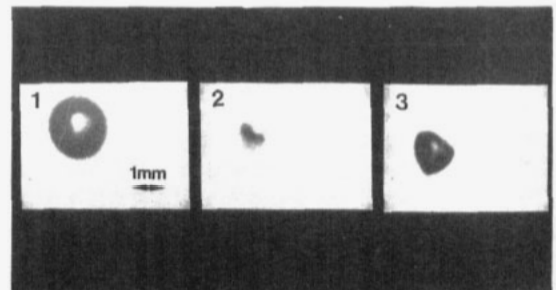


Figure 6. A selection from 18 consecutive frames, filmed at 2000 fps, showing air bubbles oscillating stably in glycerine. The acoustic pressure amplitude is 3200 Pa, the static pressure 600 Pa, and the acoustic frequency 100 Hz. The number density is higher than in figure 5, and the effect is clear on the pictures: during expansion neighbouring bubbles distort each other from the spherical shape. During compression they again become non-spherical; elongation occurs in the direction of the neighbours due to Bernoulli forces.

frame 35. Measurements from this film are later compared with theory in figure 9. Figure 6 also shows a bubble in glycerine, though at a higher production rate of bubbles. The acoustic pressure amplitude is 3200 Pa and the static pressure 600 Pa. The effect is clear in the pictures: during expansion neighbouring bubbles distort each other from the spherical shape. During compression they again become non-spherical; elongation occurs in the direction of the neighbours due to Bernoulli forces. (Though the collapsed bubbles have a profile that is reminiscent of a jetting bubble, it should be noted that this is merely coincidence: no bubble involution, and therefore no jetting, has occurred.)

Figure 7 shows the collapse of a bubble in water, with an acoustic pressure amplitude of 880 Pa and a

Figure 7. This selection of three frames details the collapse of an air bubble in water, with an acoustic pressure amplitude of 880 Pa, a static pressure of 780 Pa and an acoustic frequency of 100 Hz. The bubble, which was spherical in the expanded phase (frame 1), distorts during collapse, so that at minimum volume (frame 2) it almost involutes to form a jet, giving the characteristic 'pancake shape'. As the bubble expands, the shape becomes more spherical (frame 3).



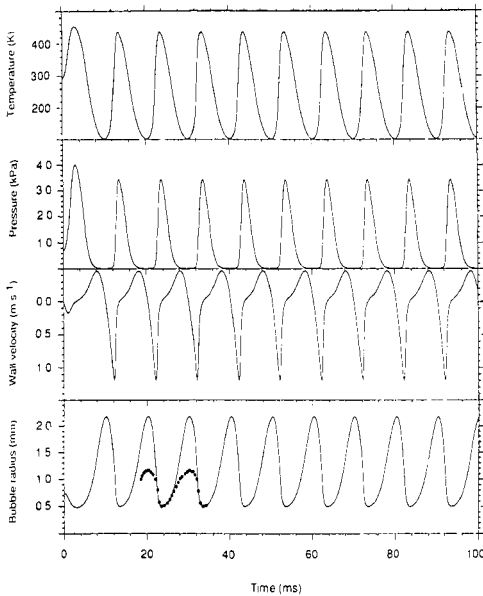


Figure 8 Experimental data (●) for bubble radius against time are plotted for comparison with the numerical solution of the Rayleigh–Plesset equation. The theoretical plots (full curves) show the radius, the velocity of the bubble wall, and the internal gas pressure and temperature, plotted against a common time axis. The air bubble, oscillating in glycerol, has an equilibrium radius of 0.75 mm. The driving force was at 100 Hz, with a pressure amplitude of 3220 Pa. The static pressure was 625 Pa, and the data for glycerol is as follows: surface tension, 0.063 N m^{-1} , density 1260 kg m^{-3} , vapour pressure, 100 Pa, dynamic viscosity, $1.487 \text{ kg m}^{-1} \text{ s}^{-1}$. The polytropic index of the gas was taken to be 1.33.

static pressure 780 Pa. The bubble, which was spherical in the expanded phase (frame 1), distorts during collapse, so that at minimum volume (frame 2) it almost involutes to form a jet, giving the characteristic ‘pancake shape’ (see, for example, Dear and Field 1988). As the bubble expands, the shape becomes more spherical (frame 3).

From photographic series where the bubble remains approximately spherical, the radius–time data were extracted and compared with the Rayleigh–Plesset predictions. Three examples are shown in figures 8, 9 and 10. The full curves show the numerical prediction, and the experimental data points are superimposed. An intermediate pressure amplitude of above five times the static value was employed for figure 8, which shows an air bubble in glycerine. The general form of the prediction agrees with the experimental data, as does the minimum radius attained by the bubble. However, the Rayleigh–Plesset solution overestimates the maximum radius by a factor of about two.

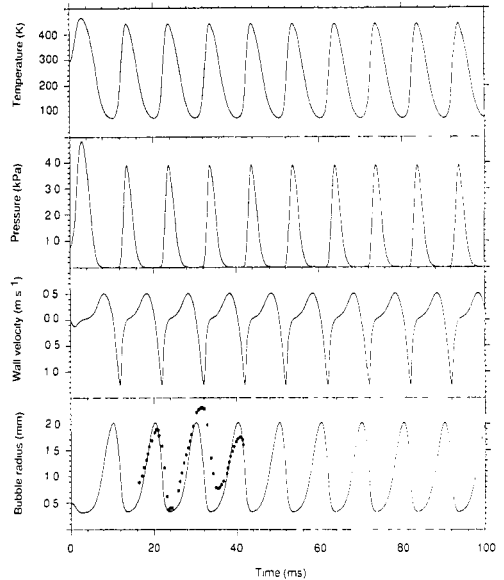


Figure 9 Plots as for figure 8 and for the sequence illustrated in figure 5, but this time for an air bubble of equilibrium radius 0.50 mm oscillating in glycerol, with a pressure amplitude of 3900 Pa and a static pressure of 600 Pa. All other values are as in figure 8.

Figure 9, which was illustrated in figure 5, is also in glycerine through the pressure amplitude is higher. The results agree well. The experimental data show the familiar half-frequency mode, in which every alternate peak has differing amplitude. This is characteristic for a bubble entering the regime of transient cavitation (Walton and Reynolds 1984). The Rayleigh–Plesset solution does not predict such behaviour for this bubble until the pressure amplitude is about 8500 Pa (compared to the 3930 Pa used here), the solutions predict that transient cavitation sets in at pressure amplitudes of around 10 kPa.

Figure 10 compares theory and experiment for a spherical air bubble in water. The absolute value of τ was extrapolated from the transit time of the bubble across the field of view, and theory and experiment agree well. The type of non-linear oscillation seen here is characteristic of a bubble of much less than resonance size when the pressure amplitude is close to the transient threshold, i.e. approaching the onset of collapse cavitation (Walton and Reynolds 1984). The two frequencies which appear in the initial stages of the motion are at the driving frequency and the resonant frequency of the bubble, the latter being stimulated by ‘shock-excitation’ (Neppiras 1980).

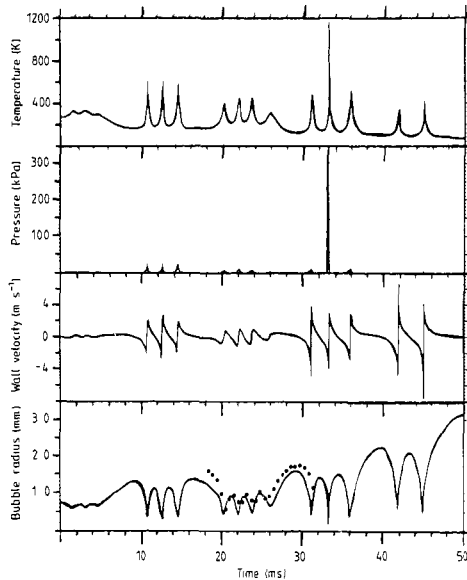


Figure 10. Experimental data (●) for bubble radius against time are plotted for comparison with the numerical solution of the Rayleigh–Plesset equation (full curves). An air bubble of equilibrium radius 0.75 mm oscillating in water, experiences a driving force at 100 Hz, with a pressure amplitude of 760 Pa. The static pressure was 785 Pa, and the data for water is as follows: surface tension, 0.0072 N m^{-2} , density 998 kg m^{-3} , vapour pressure, 0 Pa, dynamic viscosity, $10^{-3} \text{ kg m}^{-1} \text{ s}^{-1}$. The polytropic index of the gas was taken to be 1.33.

4. Discussion

The study has shown that the solutions of the Rayleigh–Plesset equation match qualitatively the observed oscillations, but the absolute values of the radii differ. Examination of the assumptions inherent in the derivation of the equation reveals some sources for the discrepancy. The criteria that must be met (Walton and Reynolds 1984) are that (a) there is a single bubble in an infinite medium, (b) at all times the bubble remains spherical, (c) spatially uniform conditions exist within the bubble, (d) the bubble radius is small compared with the acoustic wavelength, (e) no body forces (e.g. gravitational) are present, (f) bulk viscous effects can be ignored, (g) the density of the liquid is large, and its compressibility is small, compared with the values for the gas within the bubble, (h) the gas content of the bubble is constant and (i) the vapour pressure is constant during the oscillation.

The experiment described here deviates from several of these criteria, two of the assumptions in particular being clearly not met. Firstly, the bubbles are not spherical in glycerine, the assumption breaks down at high population densities and during the

collapse phase (figure 7), in water, only the smaller bubbles approximate to the spherical condition (figure 9). In the extreme case of non-sphericity, the processes of fragmentation and coalescence are beyond the scope of the equation. In addition, buoyancy forces distort the bubble shape. Secondly, the problem clearly does not involve a single bubble in an infinite medium, and so the effect of mutual Bjerknes forces, and of sound scattering by neighbouring bubbles, complicates the situation. It should be noted that the other assumptions are for the most part met. In particular, for these timescales, bulk viscous effects are negligible, so that in this regime the Rayleigh–Plesset equation is as valid as other equations (for example, that of Gilmore) which take this effect into consideration. In the higher-frequency regimes, the approximation is less valid. Therefore if the Rayleigh–Plesset equation does not accurately predict the bubble motion at these low frequencies, caution must be used when using it to predict the oscillation of bubbles at kilo- and mega-hertz frequencies.

5. Conclusions

A forced bubble in a liquid provides a good example of a non-linear driven oscillator. The apparatus is simple, and yet the use of a simulated sound field is a subtle solution to the problem that should be of interest to undergraduates. The drive system described here uses equipment readily available in most physics laboratories, and is free of the safety hazards associated with the use of high-intensity audio insonation of a liquid. Direct viewing of the bubble under stroboscopic illumination shows many of the key features of its oscillation. High-speed photography allows quantitative comparison between experiment and computed radial oscillation.

Acknowledgments

TGL thanks the SERC and Magdalene College, Cambridge, for Research Fellowships. We thank G Millar and D Johnson for technical help, and K J Fagan for his assistance with the photography. The research was supported in part by Marconi Maritime.

References

- Dear J P and Field J E 1988 *J. Fluid Mech.* **190** 409–25
- Leighton T G and Walton A J 1987 *Eur. J. Phys.* **8** 98–104
- Leighton T G, Walton A J and Pickworth M J W 1990 *Eur. Phys. J.* **11** 47–50
- Minnaert M 1933 *Phil. Mag.* **16** 235–48
- Neppiras E A 1980 *Phys. Rep.* **61** 159–251
- Pumphrey H C and Walton A J 1988 *Eur. J. Phys.* **9** 225–31
- Walton A J and Reynolds G T 1984 *Adv. Phys.* **33** 595–660